Vol. 44, No. 1 (2022) 183-197, DOI: 10.24874/ti.1078.03.21.10

Tribology in Industry

www.tribology.rs

RESEARCH

Simulation of Misaligned Journal Bearings Using Neural Networks

Kyriakos A. Kokkinidis[a], Pantelis G. Nikolakopoulos[a,*]

[a]*Machine Design Laboratory, Department of Mechanical and Aeronautical Engineering. University of Patras, Rio Patras, 26500, Greece.*

Keywords:

Journal bearings
Neural networks FDM
Misalignment

* Corresponding author:

Pantelis G. Nikolakopoulos
E-mail: pnikolakop@upatras.gr

Received: 25 March 2021
Revised: 27 April 2021
Accepted: 16 October 2021

A B S T R A C T

Utilization of smart systems, i.e. software tools that incorporate artificial intelligence (AI), in engineering applications increases. This fact is due to their ability to study the performance of complicated systems, producing results quicker and easier than typical analytical models. This article is focused on the advantages of using Artificial Neural Networks (ANNs) to solve the problem of a misaligned hydrodynamic journal bearing. Firstly, the Reynolds equation is solved using finite difference method (FDM) for different operating and misalignment conditions. The results are used to train four (4) artificial neural networks, one for each design parameter. Afterwards, the networks are tested for several operational characteristics and compared with the results of the finite difference method. The outcome is that the force and the torque can be predicted with maximum error of approximately 5% with less computational cost than the finite difference method.

1. INTRODUCTION

Misalignment in journal bearing is one of the most severe defects that influences the bearing behavior and consequentially the rotor bearing dynamics. Pressure distribution, load capacity and torque calculation has been of interest to the researchers since they are some of the most crucial parameters in the design process. Traditional methods such as finite element, finite difference, meshless methods are already being used in order to solve the Reynolds equation.

On the other hand, artificial intelligence has lately been used in tribology, trying to predict design characteristics, like pressure, friction coefficient, lubrication regions and the oil film thickness.

A CFD analysis of non-newtonian journal bearings lubrication is presented by Gertzos et al. [1]. Nuruzzaman et al. [2] investigated the pressure development and load capacity of a journal bearing using the finite element method. Moreover, the dynamics and stability of high-speed cylindrical journal bearing presented by Strzelecki [3], while a method to find the bearing's static equilibrium position was presented by Zhou et al. [4]. Kasolang et al. [5] conducted a preliminary study of pressure profile in hydrodynamic journal bearings using the FDM to solve the Reynolds equation.

König et al. [6], presented a study which predicts numerically the frictional performance of journal bearings with single- and multi-scale surface patterns of real 3D surface topographies after wearing-in in mixed-elastohydrodynamic (mixed-EHL) simulations using a multi-body simulation environment. The combination of the extended Reynolds equation with flow factors according to Patir and Cheng has been used with a deterministic asperity contact model, in order to optimize the tribological response of engineering systems.

Since misalignment is having a major impact in the performance of the journal bearing scientists studied misaligned journal bearings. The performance characteristics of misaligned journal bearings described by Jang and Khonsari [7] current studies and trends in their review paper. Nikolakopoulos and Papadopoulos studied the non-linear behavior of misaligned journal bearings [8]. A hydrodynamic analysis of misalignment journal bearings due to shaft deformation investigated by Sun and Changlin [9]. Recently, Zhang et al. [10] executed an experimental work of axial misalignment effect on the seizure load of journal bearings. Mokhtar et al. [11] presented an adiabatic solution of misaligned bearings. An investigation regarding the static and dynamic performance of misaligned journal bearing taking into account turbulent and thermohydrodynamic effects was conducted by Xu et al. [12]. Pierre et al. [13] also conducted a thermohydrodynamic study of misaligned journal bearings and compared the theoretical results with relevant experiments. Kim and Peder [14] studied the improved behavior of journal bearing operation at a large misaligned conditions with bearing flexible condition and conformable liners while Jamali and Al-Hammod [15] presented a methodology regarding the analysis of misaligned journal bearings. They solved, the Reynolds equation using the FDM. The field of artificial intelligence applied to journal bearing lubrication is relatively new and despite the already published works there is a place for future works. Rosenkranz, Marian et al. [16] provided an overview of the various application fields and methods for Artificial Intelligence (AI) and Machine Learning (ML) techniques in tribology. Wear and misalignment identification on journal bearings using ANNs was presented by Saridakis et al. [17]. The characterization of the lubrication regimes of journal bearings by machine learning (ML) presented by Moder et al. [18]. Otero et al. [19] presented the ability of ANNs to predict the friction coefficient, learn by experimental data. Ghorbanian and Ahmadi [20], presented a methodology optimization of journal bearing using ANNs and multi-objective genetic algorithms. Furthermore, Kornaev et al. [21] investigated the application of ANNs to calculate the hydrodynamic forces and the dynamic of the rotor. Canbulut et al. [22], used an ANN to predict the behavior of hydrostatic circular recessed bearings. The neural model proposed by the authors, consisted of three layers, which were one-neuron input layer, ten-neurons hidden layer, and three-neurons output layer. Results shown that the ANNs could model bearing systems in real time applications. Sinanoglue et al. [23], investigated experimentally the pressure distribution on a steel shaft supported by journal bearings, using neural networks in order to predict the bearing behavior. Badawi et al. [24], studied the influence of the geometry on the behavior of tilting pad journal bearings. They used the COMSOL Multiphysics software for the simulation of the tilting pad bearing at several eccentricity ratios and pad clearances. The outcomes were used to train the proposed ANNs. Recently, Iseli and Schiffmann [25] presented neural network regression models in order to predict the nonlinear static and linearized dynamic forces of spiral grooved gas bearings. Yang and Palazzolo [26], examined the applicability of the Reynolds equations in a thermo elastohydrodynamic titling pad journal bearing model, with ANNs. The proposed method is accurate as a CFD model, with the gain of the less computational time. According to the representative literature review above, it can be concluded that use of ANN's analyzing misaligned bearings is still missing. Hence, the main target of this research is to bridge this gap. In this paper the pressure distribution of misaligned journal bearings is calculated using the FDM. The effects of various design parameters in the bearing behavior are revealed by an intensive parametric study. Then the hydrodynamic force and torque of the oil film are calculated by integrating the pressure profile using the Simpson rule. Four (4) neural networks have been trained using the occurred results. The difference regarding the results between the numerical method and the trained artificial neural network is examined. The main purpose of this work is to illustrate that ANN's can and should be used in misaligned hydrodynamic journal bearing live monitoring systems. The reason is, that they produce results much quicker with less computational cost than the FDM and with an acceptable error. Incorporation of ANN's in such

systems could reduce their total cost (since less hardware is needed due to lower computational needs) enabling more craft shops, machine shops and factories to use them. The advantage of that would be less damages, results in bigger life times, of the bearings due to live monitoring.

2. THEORETICAL AND GEOMETRICAL CONSIDERATIONS OF MISALIGNED JOUNRAL BEARINGS

The governing equation is the Reynold's equation and can be derived either from Navier-Stokes equations (conservation of mass and momentum) or from equilibrium of an element of the fluid. The equation considering isoviscous lubricant with steady film thickness and unidirectional velocity approximations is,

$$\frac{\partial}{\partial x}\left(h^3\frac{\partial P}{\partial x}\right)+\frac{\partial}{\partial y}\left(h^3\frac{\partial P}{\partial y}\right)=6U\eta\frac{dh}{dx} \qquad (1)$$

The film thickness h is the variable that pressure distribution is affected by the most. In the next paragraphs the analytical expressions for h both for the aligned and misaligned case are presented. A typical section of the journal and the bearing for the aligned case is shown in Figure 1.

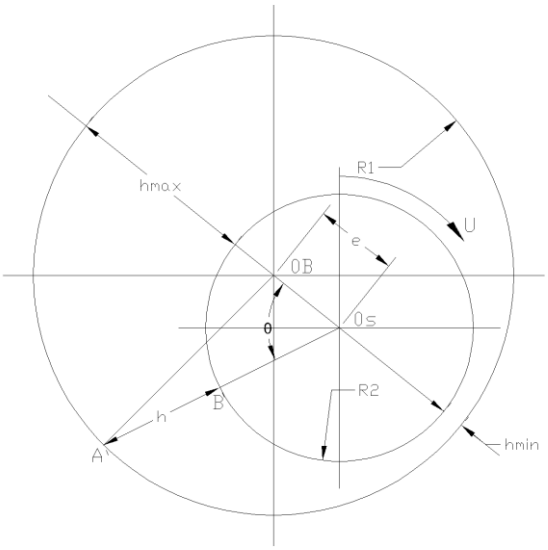

Fig. 1. Geometry of aligned journal bearing showing the oil film thickness in the bearing area.

The equation (2) that describes the oil film thickness [27] is,

$$h=e\cos\theta+R_1-R_2 \Rightarrow \\ h=e\cos\theta+c \qquad (2)$$

The sections in the x-z and y-z planes of a misaligned journal bearing are shown in Figure 2 and in Figure 3 the geometry in the x-y plane and z=0 is shown.

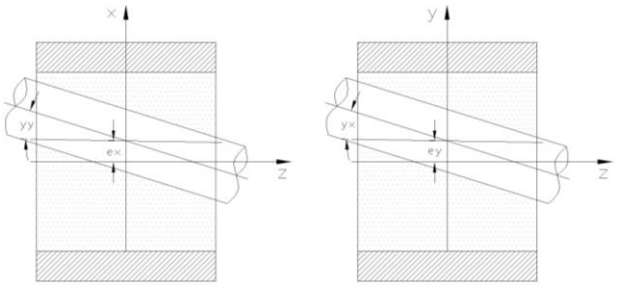

Fig. 2. Sections of misaligned journal bearing x-y and y-z planes.

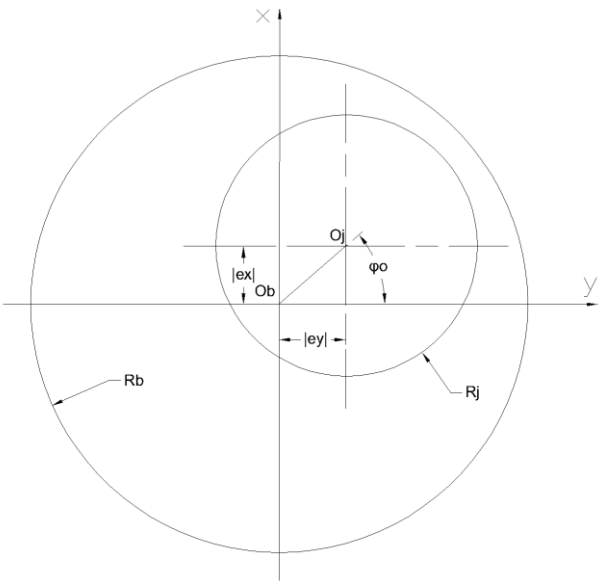

Fig. 3. Misaligned journal bearing geometry (x-y plane and z=0).

The film thickness prediction plays a crucial role in misaligned journal bearings. Nikolakopoulos et al. [8] mentioned the following expression (3) that describes the film thickness of a misaligned journal bearing:

$$h(\theta,z)=c+e_0\cdot\cos\theta+z\cdot(yy\cdot \\ \cos(\theta+\varphi_0)+yx\cdot\sin(\theta+\varphi_0)) \qquad (3)$$

Further, Joon Young Jang and Michael M. Khonsari [28] also presented a different oil film thickness equation. In the current paper the problem of isothermal hydrodynamic lubrication is considered. However, when heavy misalignment occurs then the case that needs to be studied is elastohydrodynamic lubrication, where the film thickness must be modified using the expression described analytically in [29].

The hydrodynamic forces and torques (eqs. 4-7) developed in the bearing can be evaluated [8] by integrating the hydrodynamic pressure over the bearing surface.

$$F_x = \int_0^{2\pi} \int_{-\frac{L}{2}}^{\frac{L}{2}} P(\theta, z) \cdot \cos\theta \cdot d\theta dz \qquad (4)$$

$$F_y = \int_0^{2\pi} \int_{-\frac{L}{2}}^{\frac{L}{2}} P(\theta, z) \cdot sin\theta \cdot d\theta dz \qquad (5)$$

$$M_x = \int_0^{2\pi} \int_{-\frac{L}{2}}^{\frac{L}{2}} -P(\theta, z) \cdot z \cdot \sin\theta \cdot d\theta dz \qquad (6)$$

$$M_y = \int_0^{2\pi} \int_{-\frac{L}{2}}^{\frac{L}{2}} P(\theta, z) \cdot z \cdot \cos\theta \cdot d\theta dz \qquad (7)$$

3. ARTIFICIAL NEURAL NETWORK

Artificial neural networks (ANNs) are like biological systems that consist of many nerve cells that work and masse and have the ability to learn. It is not necessary to have task-specific rules of programming an ANN. They can learn through appropriate training examples by usually applying reinforcement learning methods. A trained ANN can generalize and correlate training data on the basis of which it was trained but may also find logical solutions to similar problems in the same category for which ANN has not been trained. This means that ANN shows a high degree of tolerance for errors and data variations which is a very important comparative advantage over other learning methods that have been formulated from time to time.

An artificial neuron is a computational model that gets a set of input values ($\underset{p}{\rightarrow}$) as well as its bias (b). The dot product of the input values with the synapse weights ($\underset{w}{\rightarrow}$) plus the bias will form the input (n) of the activation function (f). The activation function may be chosen from functions such as ReLU, log-sigmoid, tan-sigmoid, linear. The output of the function (α) is transmitted to one neuron or more depending on the topology of the network. The weights involved are altered and shaped in a way that the neuron and consequently the ANN, which is made up of many neurons, can properly represent the knowledge characteristic in the training samples.

There are many different ANN types with different topologies. The one that will be used in this study is a feed-forward multilayer perceptron. The choice of the feed-forward multilayer perceptron is due to its simple nature and the accuracy of the obtained results. Fig. 4 shows a typical network of this type. The neurons and the input, output and hidden layers can be seen.

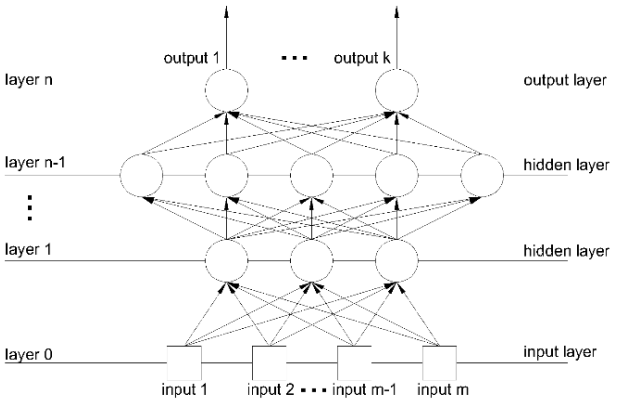

Fig. 4. Typical topology of a multilayer perceptron.

4. NUMERICAL MODEL

Equation (1) is transformed to cylindrical coordinates by setting $x = R \cdot \theta \; and \; y = z$ and the equation (8) is obtained:

$$\frac{\partial}{\partial\theta}\left(h^3 \cdot \frac{\partial P}{\partial\theta}\right) + R^2 \cdot \frac{\partial}{\partial z}\left(h^3 \cdot \frac{\partial P}{\partial z}\right) = 6 \cdot \frac{\partial h}{\partial\theta} U \cdot \eta \cdot R \qquad (8)$$

Introducing the following dimensionless parameters:

$$H = \frac{h}{c}, \mathrm{Z} = \frac{z}{L}, p = \frac{Pc^2}{6U\eta R} \qquad (9)$$

the dimensionless Reynolds equation (10) can be obtained by substituting equations (9) in equation (8):

$$\frac{\partial}{\partial\theta}\left(H^3 \cdot \frac{\partial p}{\partial\theta}\right) + \left(\frac{R}{L}\right)^2 \cdot \frac{\partial}{\partial Z}\left(H^3 \cdot \frac{\partial p}{\partial Z}\right) = \frac{dH}{d\theta} \qquad (10)$$

4.1 Finite difference method

The first and second order derivatives and equation (10) are discretized by the second order central difference scheme. The method used is the successive over-relaxation method, and pressure can be calculated by the equations (11-12).

$$p_{i,j} = \frac{A_1}{A_3} \cdot p_{i+1,j} + \frac{A_2}{A_3} \cdot p_{i-1,j} + \frac{A_4}{A_3} \cdot p_{i,j+1} + \frac{A_5}{A_3} \cdot p_{i,j-1} - \frac{B_1}{A_3} \quad (11)$$

$$\text{where } A_1 = \left(\frac{H_{i+1,j}+H_{i,j}}{2}\right)^3 \cdot \frac{1}{d\theta^2}, A_2 = \left(\frac{H_{i,j}+H_{i-1,j}}{2}\right)^3 \cdot \frac{1}{d\theta^2}, A_4 = \left(\frac{H_{i,j}+H_{i,j+1}}{2}\right)^3 \cdot \frac{1}{dZ^2} \cdot \left(\frac{R}{L}\right)^2, A_3 = A_1 + A_2 + A_4 + A_5 \text{ and } B_1 = \frac{H_{i+1,j}-H_{i-1,j}}{2 \cdot d\theta} \quad (12)$$

The boundary conditions can be concluded as in equation (13):

$$p(1,1{:}n_z) = 0 \qquad p(n_\theta, 1{:}n_z) = 0 \qquad p(i,j) = 0, p(i,j) < 0 \ (half\ Sommerfeld) \quad (13)$$

The convergence criteria that was used is described in equation (14):

$$error = max\left(\left|\frac{p - p_{old}}{p}\right|\right) \leq 10^{-7} \quad (14)$$

Where the pressure solution p is obtained as:

$$p = \omega \cdot p + (1 - \omega) \cdot p_{old} \quad (15)$$

and p_{old} are the pressure values from the previous iteration and $\omega = 1.9$. The value of ω was found through a trial and error process aiming to minimize the time needed for the method to converge.

4.2 Artificial neural networks

Artificial neural networks were suggested in order to obtain the hydrodynamic forces and torques as outputs to the input data. The input data are the misalignment angles, the eccentricity ratio, the rotational speed and the oil viscosity. The proposed ANN's are trained using input and output data from the FDM. FDM was selected, since it's a well-known, relative fast and accurate method in order to create a big number of samples. Of course, other numerical methods can be used, such finite elements [8], computational fluid dynamics [1] or meshless [30] in order to compare the results with the proposed method. The trained networks can assist the bearings designers to predict fast and easily the outputs for not included in the training procedure input values. The severity of misalignment can be defined by the hydrodynamic forces and torques developed in the bearing. This is the reason why the outputs of the networks were chosen to be the hydrodynamic torques and forces acting along the x and y axes. The number of ANNs that is used is four (4). One (1) for each force and torque component. One network per design variable was used in order to avoid the complexity of one network including all four (4) output variables. The network topologies are different between the ANNs in forces calculation and those that were used in torques calculation. The following tables display the characteristics for each one.

Table 1. ANN (forces) characteristics.

ANN (FORCES)	
No of hidden layers:	1
No of neurons in the hidden layer:	30
No of neurons in the input layer (inputs):	5
No of neurons in the output layer (outputs):	1
Activation function:	logsig
No of training samples:	248832
No of epochs to end training:	1000

Table 2. ANN (torques) characteristics.

ANN (TORQUES)	
No of hidden layers:	2
No of neurons in the input layer (inputs):	5
No of neurons in the first hidden layer:	30
No of neurons in the second hidden layer:	5
No of neurons in the output layer (outputs):	1
Activation function first hidden layer:	logsig
Activation function second hidden layer:	tansig
No of training samples:	248832
No of epochs to end training:	1000

Different topologies have been examined in order to decide the suitable for the certain problem. The outcome of the investigation is presented in figure 5. The case of 35 neurons was selected due to small error and less training time.

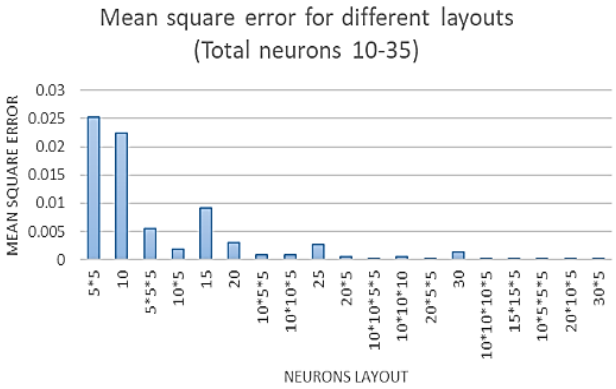

Fig. 5. Mean square error for different layouts and different total number of neurons.

Figure 6 shows the logic and the process behind the current work extended in a live monitoring environment.

Table 4 contains the range of each input variable that was used to create the training data. From each variable range twelve (12) values were chosen. All the possible combinations for the input data are $12^5 = 248832$.

Table 3. Mean square error and training time for different topologies of the ANN.

Layout	Training Time	Mean square error
5	120	0.28934
5*5	201	0.02519
10	174	0.022369
5*5*5	281	0.005514
10*5	287	0.0018738
15	236	0.0090852
20	306	0.0030219
10*5*5	393	0.00085287
10*10*5	564	0.00080137
25	397	0.0027449
20*5	538	0.0004736
10*10*5*5	676	0.00018823
10*10*10	741	0.00049467
20*5*5	651	0.00023139
30	490	0.0013611
10*10*10*5	932	0.0001409
15*15*5	1140	8.94E-05
10*5*5*5	798	0.00024993
20*10*5	1054	6.60E-05
30*5	981	0.00012516

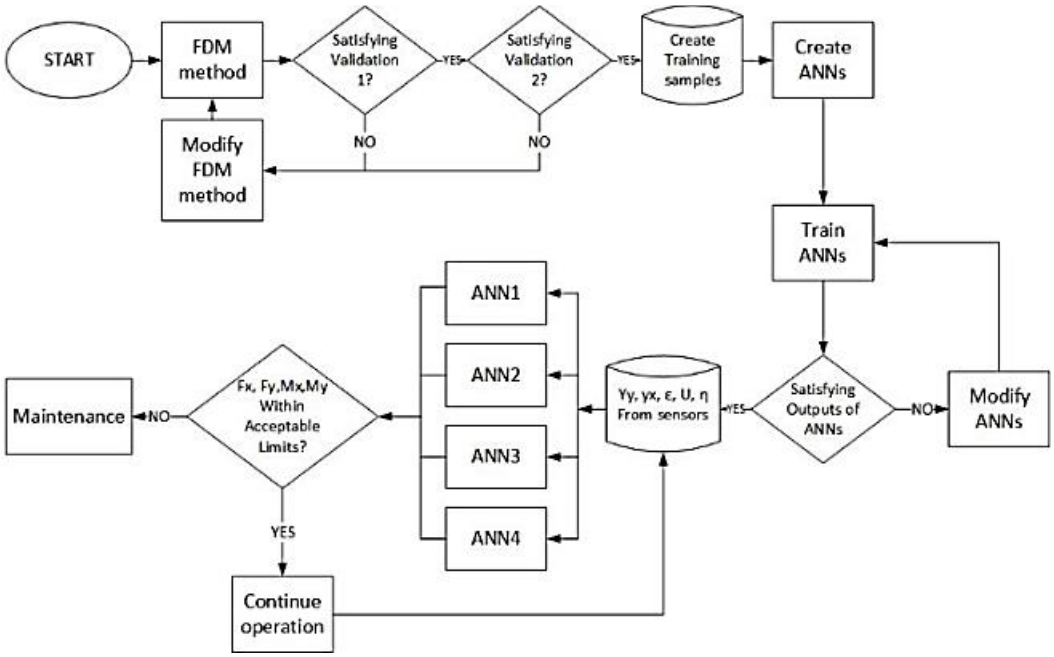

Fig. 6. Current work flowchart extended in a live monitoring environment.

Table 4. Range of input values.

Input variable	Min value	Max value	Unit
yx	0	0.1	(°)
yy	0	0.1	(°)
ε	0.05	0.3	(-)
η	0.020	0.040	(Pas)
U	5	10	(m/s)

The min and max values of the variables were chosen to describe typical working conditions of a misaligned journal bearing. The range of U is referred to a shaft rotational speed of ≈ 1600-3200 rpm, the range of η corresponds to working temperature ≈ 30-60 °C and the combination of yx, yy and ε ranges were chosen

in order to avoid shaft and bearing contact. In actual industrial applications the engineer has to define the range according to the working conditions of the factory's specific machines. The tighter the range, the better the results of the training of the ANN will be.

The outputs were produced using the FDM method for each one of the 248832 random set of parameters within the above range. The known inputs and outputs are the training data. Once the network is trained it can produce outputs depending on the random inputs that it gets. The training samples have the following form:

ANN 1

$$\begin{bmatrix} yx & yy & \varepsilon & U & \eta & F_x \\ \vdots & \vdots & \vdots & \vdots & \vdots & \vdots \end{bmatrix}_{248,832\times 6}$$

ANN 2

$$\begin{bmatrix} yx & yy & \varepsilon & U & \eta & F_y \\ \vdots & \vdots & \vdots & \vdots & \vdots & \vdots \end{bmatrix}_{248,832\times 6}$$

ANN 3

$$\begin{bmatrix} yx & yy & \varepsilon & U & \eta & M_x \\ \vdots & \vdots & \vdots & \vdots & \vdots & \vdots \end{bmatrix}_{248,832\times 6}$$

ANN 4

$$\begin{bmatrix} yx & yy & \varepsilon & U & \eta & M_y \\ \vdots & \vdots & \vdots & \vdots & \vdots & \vdots \end{bmatrix}_{248,832\times 6}$$

Note that the first five (5) columns are the known inputs and the last column is the known output.

4.3 Validation of the FDM numerical model

ANNs will produce results according to the training sample that is given. It is understandable that, if the training samples are not correct the results will not be correct either. For this reason, the FDM that used to create the results was tested meticulously to ensure that the training samples are correct. Figure 7 shows the attitude angle vs L/D ratio and attitude angle vs dimensionless eccentricity of a short aligned journal bearing. They are calculated using the analytical equations given by Stachowiak and Batchelor [27] and the FDM method used in the current work. This ensures that FDM code gives accurate results for the pressure distribution of an aligned journal bearing since attitude angle is dependent on pressure distribution calculation. The code for the Simpson numerical integration gives accurate results since attitude angle calculation is dependent on pressure integration over the bearing area to calculate the hydrodynamic forces.

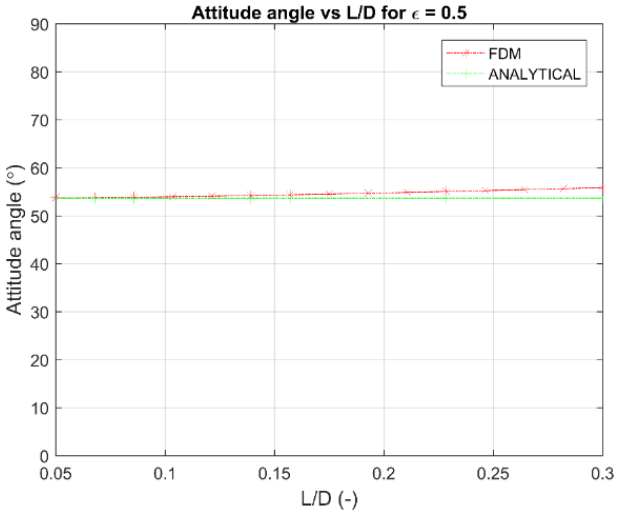

(a)

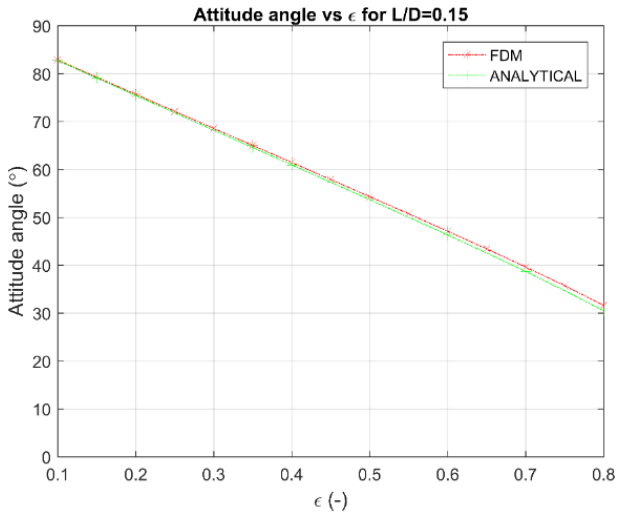

(b)

Fig. 7. (a) Attitude angle vs L/D for short aligned journal bearing (Stachowiak [27] & current work) calculated with FDM method and analytical method. (b) Attitude angle vs $\boldsymbol{\varepsilon}$ for short aligned journal bearing (Stachowiak[27] & current work) calculated with FDM method and analytical method.

Table 5 and Table 6 are the second step of validation. Table 5 shows the used characteristics of the journal bearing for the validation. Table 6 contains the values of maximum pressure between current work and the work of Sun and Changlin [9]. Sun and Changlin [9] used Reynolds boundary condition whereas in the current work half Sommerfeld boundary condition was used. Reynolds condition produces accurate results in the cavitation region. However, the computational cost increases. This leads to

exponential increase in the total computational cost since 248832 samples must be created. The difference between those two boundary conditions is expected to be around 10 %. This is confirmed as seen in Table 5. Variables α, γ, ψ_0 are defined by Sun and Changlin [9]. This step of validation ensures that the pressure distribution of a misaligned journal bearing is accurately calculated.

Table 5. Journal bearing characteristics used for validation.

Variable	Value	Unit
R	30	(mm)
L	66	(mm)
c	0.03	(mm)
n	3000	(rpm)
η	0.009	(Pas)

Table 6. P_{max} comparison between current work and Sun et al. [9].

Test No.	α (°)	γ (°)	ψ0 (°)	Pmax (MPa),Sun et al. [9]	Pmax Current work (MPa)	Difference (%)
1	0	0	0	33.06	28.89	**12.6**
2	0	0	0.004	39.6	34.55	**12.8**
3	0	0	0.007	63.58	55.7	**12.4**
4	0	0	0.01	415.35	373.65	**10.0**
5	90	90	0	33.06	29.17	**11.8**
6	90	90	0.01	32.95	29.12	**11.6**
7	90	90	0.02	34.95	32.04	**8.3**
8	90	90	0.03	143.34	133.28	**7.0**

By combining the two (2) steps of validation it can be said with certainty that the pressure distribution of a misaligned journal bearing is calculated correctly and that the code that is used for the two (2) dimensional numerical integration using the Simpson rule does not have any errors.

5. RESULTS AND DISCUSSION

5.1 Sense of the obtained results

The present analysis presents a computational frame work based on Reynolds equation for simulating misaligned journal bearings using ANNs. Comparisons with the FDM are also done in order to validate and to teach the proposed network. Both ANN and FMD algorithms have been developed, validated and compered in the frame of this paper.

Table 7. Input variables constant values used to produce the results.

Variable	Value	Unit
yx	0.07	(°)
yy	0.07	(°)
ε0	0.15	(-)
η	0.030	(Pas)
U	7	(m/s)

For each trained ANN, its output value $(F_x/F_y/M_x/M_y)_{ANN}$ is compared to the output value of the FDM $(F_x/F_y/M_x/M_y)_{FDM}$, as a function of each input variable $(yx/yy/\varepsilon_0/\eta/U)$ separately. Forces and moments are very significant parameters as well as the misalignment angles in order to characterize a misaligned journal bearing [28]. This is achieved by changing the value of one of the input variables $(yx/yy/\varepsilon_0/\eta/U)$ and keeping the others constant. Table 7 shows the constant values of the variables that were used to produce the results. For every diagram the four input variables get the constant value of Table 7 and one gets random values within the range that was used in the training phase (Table 4). It is of importance to note that these random values are not the values used for the training although a few of them might be coincident. To make it clearer the range for U variable is between 5 and 10m/s. In the training phase twelve (12) values were chosen within that range whereas in the results phase fifty (50) values were tested. Next to each diagram the error variation between the FDM and the ANN is shown. The total number of the obtained diagrams are forty (40). However, the main aim of this work is to prove and show that ANNs can produce results faster and with good enough accuracy compared to the FDM method. That is why not all forty (40) diagrams are presented.

5.2 Error analysis

Error analysis, is also a very important task, in order to show the sensitivity [16] and the accuracy of the neural networks against the traditional solution methods such us FDM. This helps in proving that the ANN is robust and its topology is well selected. Table 8 shows the minimum and maximum error value for all forty (40) diagrams which is of importance. Besides that, ten (10) of them are chosen to be presented. One (1) for each input variable $(yx/yy/\varepsilon_0/\eta/U)$ with one of the hydrodynamic torques or forces $(F_x/F_y/M_x/M_y)$ and its error diagram. More specifically the $M_y - yx, M_x - yy, F_y - \varepsilon_0, F_y - \eta$ *and* $F_x - U$ and their error diagrams are presented. Errors are crucial for both small misalignment angles, or for higher ones, especially since misalignment angles are used to predict the dynamics and the stability [28] of journal bearings. Dynamics and stability are also influenced by the produced forces and couples [31,32]. Lastly, a comparative diagram for calculation time needed between FDM and ANN method is presented. The last diagram (Figure 13) is the one that proves the "produce results faster" claim whereas Table 8 and Figure 8 - Figure 12 prove the "produce results with good enough accuracy" claim. Solution time also plays a significant role in a possible online monitoring system [33].

Figure 8 shows the torque acting along the y-direction vs misalignment angle *yx* obtained by ANNs and FDM method. The absolute value of the magnitude of the torque increases for an increase in misalignment angle *yx.* The error's minimum value is 4.22% and its maximum is 4.65% and generally decreases with increase in misalignment angle *yx.* The increase of the magnitude can be explained by the hydrodynamic wedge effect. The value of the minimum film thickness decreases as yx increases. This creates higher pressure values resulting to higher force and consequently torque values.

Figure 9 is similar to Figure 8 and shows the torque acting along the x-direction vs misalignment angle *yy* obtained by ANNs and FDM method. In this case the error values are slightly higher than previously. The minimum value is 4.48% and the maximum is 4.69% and generally decreases with increase in misalignment angle *yy*. There is also a difference in the torque's magnitude values. In Figure 8 the minimum torque value is 10 Nm and the maximum is 26 Nm whereas in Figure 11 the minimum is 19 Nm and the maximum is 34 Nm. How can this be explained however since the value of the min film thickness in this case is not smaller than the value of the previous case? The answer is that the pressure distribution is formed in a way that the hydrodynamic force F is acting at an angle such that the resulting component F_y is greater than the F_x component.

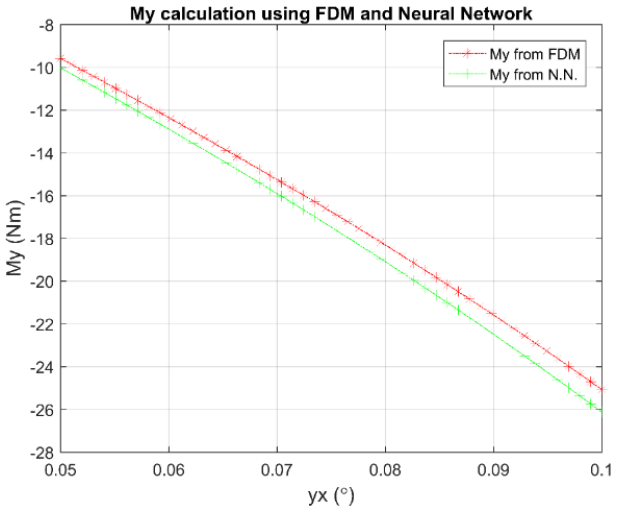

(a)

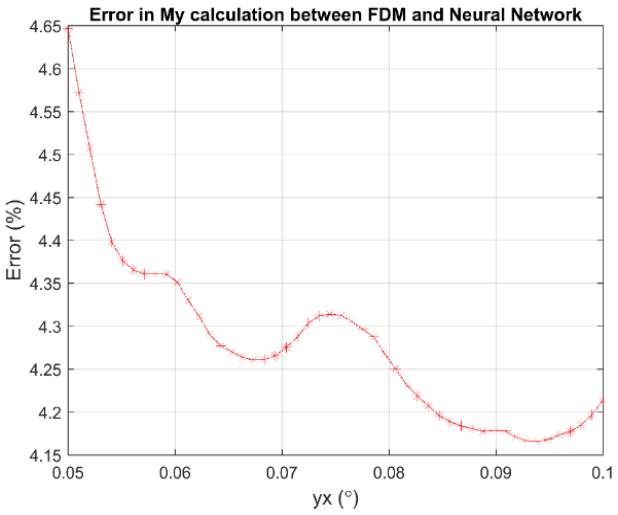

(b)

Fig. 8. (a) Hydrodynamic torque acting along the y-axis vs misalignment angle *yx* extracted with ANNs and FDM. (b) Error of the hydrodynamic torque acting along the y-axis vs misalignment angle *yx* calculation between ANNs and FDM methods.

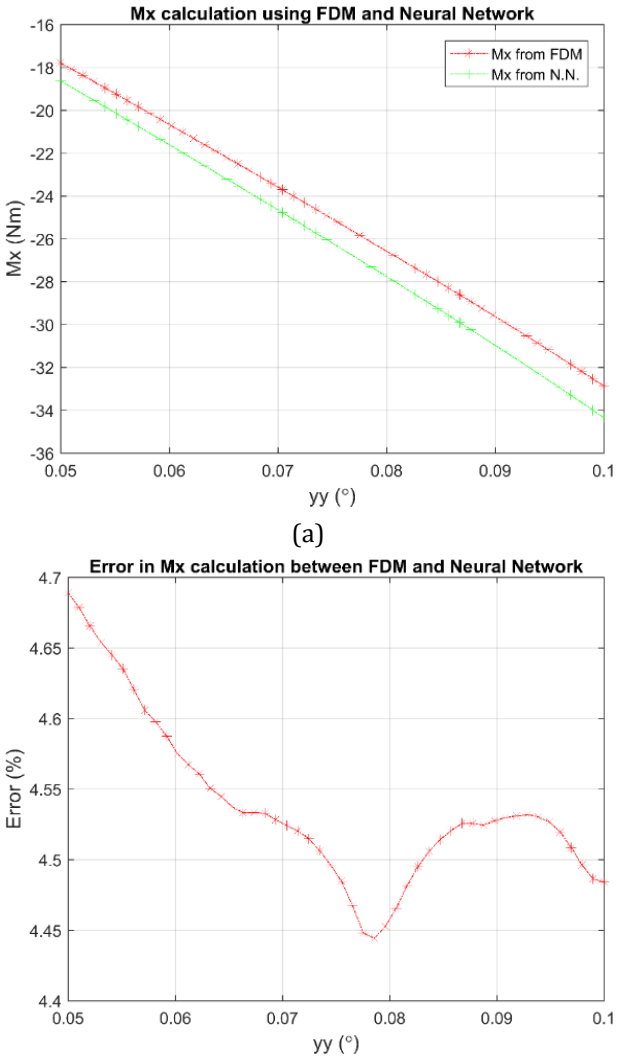

Fig. 9. (a) Hydrodynamic torque acting along the x-axis vs misalignment angle yy extracted with ANNs and FDM. (b) Error of the hydrodynamic torque acting along the x-axis vs misalignment angle yy calculation between ANNs and FDM methods.

The resulting hydrodynamic force component acting on the y-direction vs dimensionless eccentricity ε_0 obtained by ANNs and FDM method is shown in Figure 10. The magnitude of the force increases for an increase in eccentricity ε_0. As eccentricity increases the shaft is closer to the bearing resulting to reduced minimum film thickness. As minimum film thickness decreases the pressure values increase. Increased pressure values mean increase in F_y value since F_y is calculated by integrating the pressure distribution. Error's minimum value is 3.554% and its maximum is 3.88% and generally decreases with increase in eccentricity ε_0. What is interesting however is that the error distribution at the part of the diagram corresponding eccentricity ratios between 0.05 and 0.1 is completely irregular whereas for eccentricity ratios greater than 0.1 the distribution is smoother. The reason for this could be the fact that for such small eccentricities the shaft and the bearing are almost concentric. This means that the film thickness does not vary a lot and its value is close to the shaft clearance. In this case the analysis is more accurate using Petroff's theory.

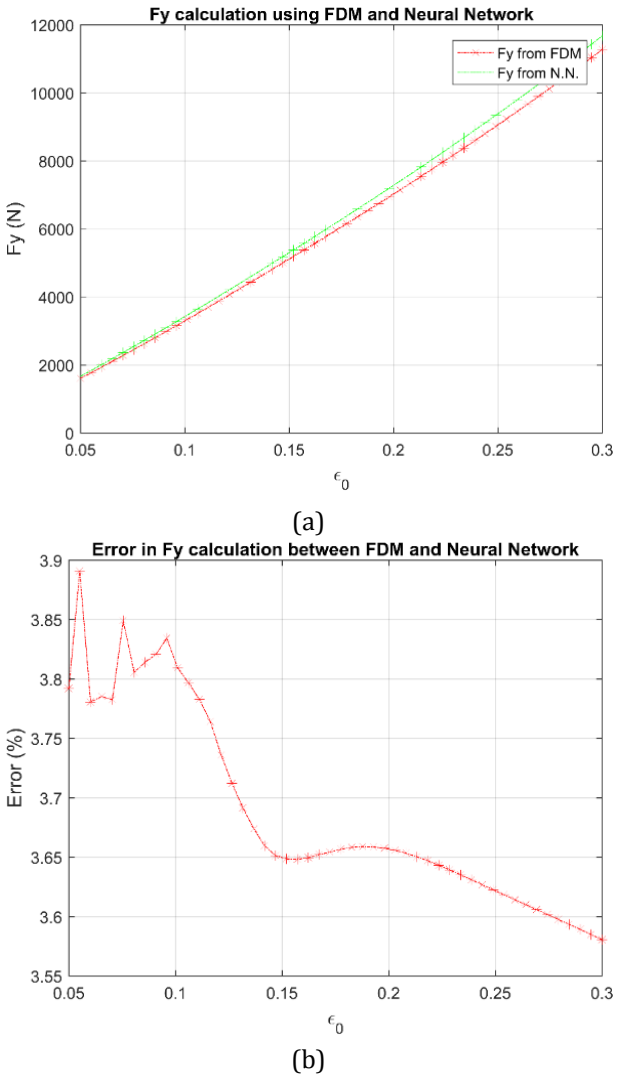

Fig. 10. (a) Hydrodynamic force acting along the y-axis vs dimensionless eccentricity ε_0 extracted with ANNs and FDM. (b) Error of the hydrodynamic force acting along the y-axis vs dimensionless eccentricity ε_0 calculation between ANNs and FDM methods.

Figure 11 shows the resulting hydrodynamic force component acting on the y-direction vs viscosity η obtained by ANNs and FDM method. The magnitude of the force increases linearly for an increase in viscosity η. The error's minimum value is 3.628% and its maximum is 3.653%. The

error decreases, then increases and then decreases again with increase in viscosity η. This linear increase is not unexpected. The pressure distribution for the short bearing approximation [27] is given by the equation (16):

$$\begin{aligned} \mathrm{p} &= \frac{dh}{dx} \cdot \left(y^2 - \frac{L^2}{4} \right) \cdot \frac{3 \cdot U}{h^3} \cdot \eta \\ &= C \cdot \eta \; if \; C \\ &= \frac{dh}{dx} \cdot \left(y^2 - \frac{L^2}{4} \right) \cdot \frac{3 \cdot U}{h^3} \end{aligned} \tag{16}$$

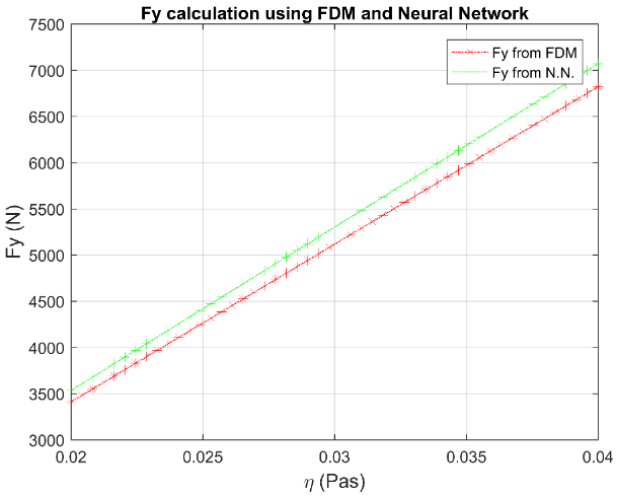

(a)

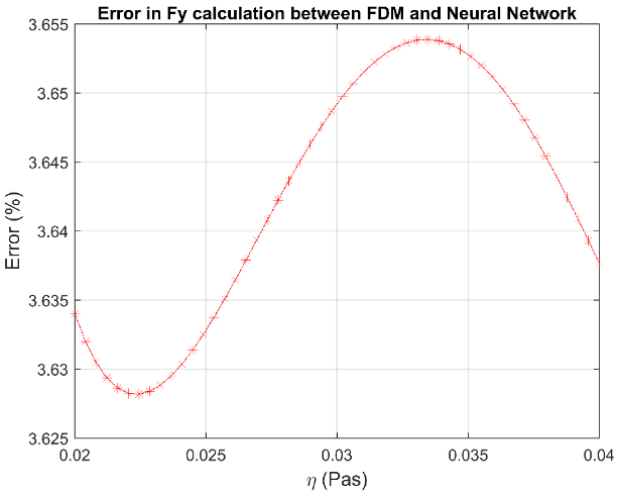

(b)

Fig. 11. (a) Hydrodynamic force acting along the y-axis vs dynamic viscosity η extracted with ANNs and FDM. (b) Error of the hydrodynamic force acting along the y-axis vs dynamic viscosity η calculation between ANNs and FDM methods.

The above equation (16) is far from accurate for the case studied in the current work. However, it is very useful to get an approximation of how each variable affects the pressure distribution. In the above equation there is a linearity between η and p. Another thing to be noticed is that the error's distribution is sinusoidal. The authors attribute it to a couple of possible reasons, but it is still under investigation. The main assumption is that this has to do with the linear correlation between η and p and the way calculations are performed inside the network.

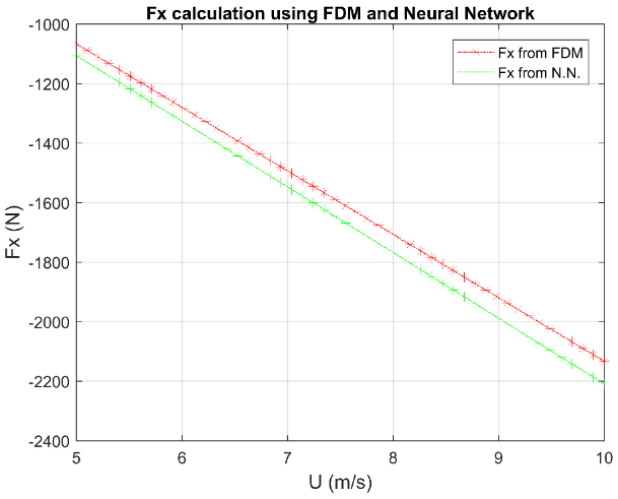

(a)

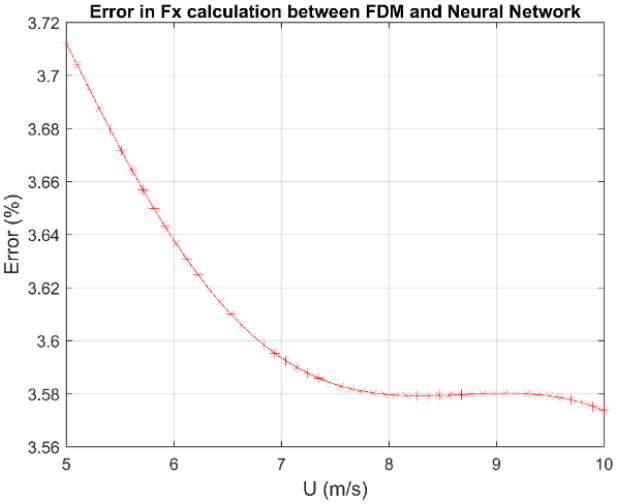

(b)

Fig. 12. (a) Hydrodynamic force acting along the x-axis vs circumferential velocity U extracted with ANNs and FDM. (b) Error of the hydrodynamic force acting along the x-axis vs circumferential velocity U calculation between ANNs and FDM methods.

The resulting hydrodynamic force component acting on the x-direction vs linear speed of the shaft's outer surface U obtained by ANNs and FDM method is shown in Figure 12. The magnitude of the force increases linearly for an increase in speed U. The error's minimum value is 3.57% and its maximum is 3.71% and decreases with increase in speed U. As U increases pressure distribution also increases

resulting to increase in hydrodynamic force. The force is acting along the negative side of the x-axis with magnitude equal to the absolute value of the force. That is the reason why negative values occur in the diagram.

As stated earlier only the above diagrams will be presented. The minimum and maximum error values for both the diagrams that were presented here and those that were not presented are in Table 8.

There is a very good agreement between the values attained by the ANN and those calculated by the FDM method. The minimum error is 3.050 % and the maximum is 4.910 %.

Table 8. Minimum and maximum error value in hydrodynamic force and torque calculation between FDM method and ANNs.

Variable	F_x *err* (%)		F_y *err* (%)		M_x *err* (%)		M_y *error* (%)	
	min	max	min	max	min	max	min	max
yx	3.05	3.82	3.762	3.834	4.340	4.540	4.220	4.650
yy	3.31	3.95	3.720	3.840	4.480	4.690	4.120	4.447
ε_0	3.20	3.72	3.554	3.880	4.400	4.850	4.200	4.390
η	3.59	3.69	3.628	3.653	4.790	4.910	4.274	4.285
U	3.57	3.71	3.636	3.652	4.806	4.850	4.257	4.287

Figure 13 shows that the computational time needed for the FDM method is many times longer than this of the trained ANN. This difference increases with an increase in the mesh nodes. In the actual simulation with the number of nodes used to obtained the results and train the network, the difference was so big that it was not visually clear in the diagram. In Figure 13 the number of nodes was reduced until the difference is clear in the diagram. The computer characteristics used for the calculations is not of importance since the goal is to make a comparison between the two (2) methods.

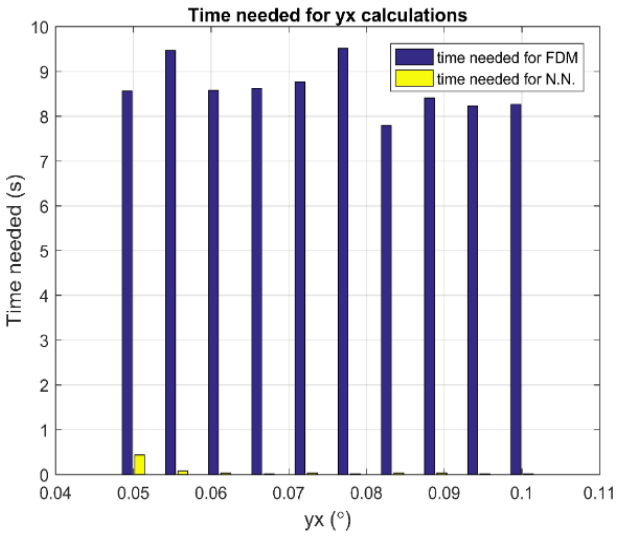

Fig. 13. Calculations time comparison between ANNs and FDM method.

The solution time and the error between ANNs and a traditional method such as FDM, suggest that the results are very promising for the use of ANNs in order to simulate misaligned journal bearings and also to predict the behavior of several operational characteristics. The faster the results of the network the easier it becomes for the network to be used in online monitoring systems. The higher the accuracy of the network the more suitable it becomes to use the network in online monitoring systems.

6. CONCLUSIONS

This work resulted in some important conclusions regarding the application of ANNs to the tribological design of misaligned journal bearings. The rarity of similar works in scientific literature gives more weight to the results and opens a new field of research. It was found that a satisfactory prediction can be made (maximum error≅5%) regarding the values of hydrodynamic forces and torques action on a misaligned shaft. More specifically, the following are observed:

1. The error fluctuates without a specific pattern but within acceptable limits.
2. Maximum appears in most cases in the max or min values of the input variables.
3. The minimum error value in forces calculation is 3.05% and the maximum is 3.95 and appear in F_x *vs* yx and F_y *vs* yy diagrams respectively.

4. The minimum error value in torques calculation is 4.12% and the maximum is 4.91 and appear in $M_y\ vs\ yy$ and $M_y\ vs\ \eta$ diagrams respectively.
5. The maximum error value in all cases is 4.91% and appears in $M_x\ vs\ \eta$ diagram.
6. The results of the trained ANNs are satisfying only for the values of input variables within the range used in the training.
7. Computational cost of the ANN is less compared to the FDM.

As a generic conclusion, the proposed methodology with the ANNs can be used to solve the Reynolds equation of misaligned journal bearings with high accuracy and low computational cost. This is very helpful tool in order to solve problems in hydrodynamic lubrication of misaligned bearings, compared to conventional approaches.

REFERENCES

[1] K. Gertzos, P.G Nikolakopoulos, C.A. Papadopoulos, *CFD analysis of journal bearing hydrodynamic lubrication by Bingham lubricant*, Tribology International, vol. 41, iss. 12, pp. 1190-1204, 2008, doi: 10.1016/j.triboint.2008.03.002

[2] D. Nuruzzaman, M. Khalil, M. Chowdhury, M. Rahaman, *Study on pressure distribution and load capacity of a journal bearing using finite element method and analytical method*, International Journal of Mechanical & Mechatronics Engineering IJMME-IJENS, vol. 10, no. 5, pp. 1-8, 2010.

[3] S. Strzelecki, *Dynamic Characteristics and Stability of High Speed Cylindrical Journal Bearing*, Vibrations in Physical Systems , vol. 29, no. 9, pp. 1-9, 2018.

[4] W. Zhou, X. Wei, L. Wang, G. Wu, A *superlinear iteration method for calculation of finite length journal bearing's static equilibrium position*, Royal Society Open Science, vol. 4, no. 5, pp. 161059, 2017, doi:10.1098/rsos.161059

[5] S. Kasolanga, M. Ahmada, R. Joyceb, C. Taib, *Preliminary study of Pressure Profile in Hydrodynamic Lubrication Journal Bearing*, Proccedia Engineering, vol. 41, pp. 1743-1749, 2012, doi: 10.1016/j.proeng.2012.07.377

[6] F. König, A. Rosenkranz, P.G. Grützmacher, F. Mücklich, G. Jacobs, *Effect of single-and multi-scale surface patterns on the frictional performance of journal bearings–A numerical study*, Tribology International, vol. 143, Available online, 2020, doi: 10.1016/j.triboint.2019.106041

[7] J. Jang, M. Khonsari, *On the Characteristics of Misaligned Journal Bearings*, Lubricants, vol. 3, iss. 1, pp. 27-53, 2015, doi: 10.3390/lubricants3010027

[8] P.G. Nikolakopoulos, C.A. Papadopoulos, *Non-linearities in misaligned journal bearings*, Tribology International, vol. 27, iss. 4, pp. 243-257, 1994, doi: 10.1016/0301-679X(94)90004-3.

[9] J. Sun, G. Changlin, *Hydrodynamic lubrication analysis of journal bearing considering misalignment caused by shaft deformation*, Tribology International, vol. 37, iss. 10, pp. 841-848, 2004, doi: 10.1016/j.triboint.2004.05.007.

[10] X. Zhang , Z. Yin, Q. Dong, *An experimental study of axial misalignment effect on seizure load of journal bearings*, Tribology International, vol. 131, pp. 476-487, 2019, doi: 10.1016/j.triboint.2018.11.014

[11] M. Mokhtar, Z. Safar, M. Abd-EI-Rahman, *An Adiabatic Solution of Misaligned Journal Bearings*, Journal of Tribology, vol. 107, iss. 2, pp. 263-267, 1985, doi: 10.1115/1.3261041

[12] G. Xu, J. Zhou, H. Geng, M. Lu, L.Yang, L. Yu, *Research on the Static and Dynamic Characteristics of Misaligned Journal Bearing Considering the Turbulent and Thermohydrodynamic Effects*, Journal of Tribology, vol. 137, iss. 2, pp. 1-8, 2015, doi: 10.1115/1.4029333

[13] I. Pierre, J. Bouyer, M. Fillon, *Thermohydrodynamic Study of Misaligned Plain Journal Bearings - Comparison Between Experimental Data and Theoretical Results*, International Journal of Applied Mechanics and Engineering, vol. 7, no. 3, pp. 949-960, 2002.

[14] T. Kim , K. Pede, *Improvement of journal bearing operation at heavy misalignment using bearing flexibility and compliant liners*, Journal of Engineering Tribology, vol. 226, iss. 8, pp. 651-660, 2018, doi: 10.1177/1350650112439372.

[15] H. Jamali, A. Al-Hammod, *A New Method for the Analysis of Misaligned Journal Bearing, Tribology in Industry*, vol. 40, no. 2, pp. 213-224, 2018, doi: 10.24874/ti.2018.40.02.05

[16] A. Rosenkranz, M. Marian, F. Profito, N. Aragon, R. Shah, *The use of Artificial Intelligence in Tribology-A perspective*, Lubricants, vol. 9, iss. 1, 2021, doi: 10.3390/lubricants9010002

[17] K. Saridakis, P. Nikolakopoulos, C. Papadopoulos, A. Dentsoras, *Identification of wear and misalignment on journal bearings using artificial neural networks,* Proceedings of the Institution of Mechanical Engineers, Part J: Journal of Engineering Tribology, vol. 226, iss. 1, pp. 208-210, 2011, doi: 10.1177/1350650111424237

[18] J. Moder, P. Bergmann, F. Grün, *Lubrication Regime Classification of Hydrodynamic Journal Bearings by Machine Learning Using Torque Data*, Lubricants, vol. 6, iss. 4, pp. 1-15, 2018, doi: 10.3390/lubricants6040108

[19] J. Echávarri Otero, E. De la Guerra Ochoa, E. Chacón Tanarro, P. Lafont Morgado, A. Díaz Lantada, J.M. Munoz-Guijosa, J.L. Muñoz Sanz, *Artificial neural network approach to predict the lubricated friction coefficient*, Lubrication science, vol. 26, iss. 3, pp.141-162, 2014, doi: 10.1002/ls.1238

[20] J. Ghorbanian, M. Ahmad, *Design predictive tool and optimization of journal bearing using neural network model and multi-objective genetic algorithm*, Scientia Iranica, vol. 18, iss. 5, pp. 1095-1105, 2011, doi: 10.1016/j.scient.2011.08.007

[21] A. Kornaev, N. Kornaev, E. Kornaeva, A. Savin, *Application of Artificial Neural Networks to Calculation of Oil Film Reaction Forces and Dynamics of Rotors on Journal Bearings*, International Journal of Rotating Machinery vol. 2017, pp. 1-11, 2017, doi: 10.1155/2017/9196701

[22] F. Canbulut, S. Yildirim, C. Sinanoglu, *Design of artificial neural network model for analysis of frictional power loss of hydrostatic slipper bearing*, Tribology Letters, vol. 17, pp. 887–899, 2004, doi: 10.1007/s11249-004-8097-6

[23] C. Sinanoglu, A.O. Kurban, S. Yildirim, *Analysis of pressure variations on journal bearing system using artificial neural network*, Industrial Lubrivation and Tribology, vol. 56, iss. 2, pp. 74–87, 2004, doi: 10.1108/00368790410524038

[24] M.B. Badawi, W.A. Crosby, I.M. El Fahham, M.H. Alkomy, *Performance analysis of tilting pad journal bearing using COMSOL Multiphysics and Neural Networks*, Alexandria Engineering Journal, vol. 59, iss. 2, pp. 865-881, 2020, doi: 10.1016/j.aej.2020.03.015

[25] E. Iseli, J. Schiffmann, *Prediction of the reaction forces of spiral-groove gas journal bearings by artificial neural network regression models*, Journal of Computational Science, vol. 48, Available online, 2021, doi: 10.1016/j.jocs.2020.101256

[26] J. Yang, A. Palazzolo, *Computational fluid dynamics based mixing prediction for tilt pad journal bearing TEHD modeling - Part II: Implementation with machine learning*, Journal of Tribology, vol. 143, iss. 1, pp. 1-18, 2021, doi: 10.1115/1.4047751.

[27] G.W. Stachowiak, A.W. Batchelor, *Engineering Tribology*, 3rd Edition, Butterworth Heinemann, 2005.

[28] J.Y. Jang, M.M. Khonsari, *On the Characteristics of Misaligned Journal Bearings*, Lubricants, vol. 3, iss. 3, pp. 27-53, 2015, doi: 10.3390/lubricants3010027

[29] M. Marian, M. Bartz, S. Wartzack, A. Rosenkranz, *Non-Dimensional Groups, Film Thickness Equations and Correction Factors for Elastohydrodynamic Lubrication: A Review*, Lubricants, vol. 8, iss. 10, pp. 1-20, 2020, doi: 10.3390/lubricants8100095

[30] R. Niccoleti, *Comparison Between a Meshless Method and the Finite Difference Method for Solving the Reynolds Equation in Finite Bearings*, Journal of Tribology, vol. 135, iss. 4, pp. 1-9, 2013, doi: 10.1115/1.4024752

[31] K.M. Abdou, E. Saber, *Effect of rotor misalignment on stability of journal bearings with finite width*, Alexandria Engineering Journal, vol. 59, iss. 5, pp. 3407-3417, 2020, doi: 10.1016/j.aej.2020.05.020

[32] T.V.V.L.N. Rao, *Stability Characteristics of Misaligned Journal Bearing*, Advances in Vibration Engineering, vol. 11, no. 4, pp. 361-369, 2012.

[33] A. Simm, Q. Wang, S. Huang, W. Zhao, *Laser based measurement for the monitoring of shaft misalignment*, Measurement , vol. 87, pp. 104-116, 2016, doi: 10.1016/j.measurement.2016.02.034

Nomenclature

b	neuron bias
c	radial clearance (m)
D	bearing diameter $D = 2 \cdot R_1$ (m)
e	eccentricity (m)
e_x	eccentricity on the x-axis (m)
e_y	eccentricity on the y-axis (m)
F_x	force on the journal due to lubricant pressure on the x-axis (N)
F_y	force on the journal due to lubricant pressure on the y-axis (N)
$h(\theta)$	film thickness (m)
$H(\theta)$	dimensionless film thickness
h_{max}	maximum film thickness (m)
h_{min}	minimum film thickness (m)
L	bearing length (m)
M_x	torque on the journal due to lubricant pressure on the x-axis (Nm)
M_y	torque on the journal due to lubricant pressure on the y-axis (Nm)
n_z	number of nodes in z direction
n_θ	number of nodes in θ direction
O_b	bearing center
O_s	journal center
P	lubricant pressure (Pa)

p	dimensionless pressure $p = (P \cdot c^2)/(6 \cdot U \cdot \eta \cdot R)$
$\underset{p}{\rightarrow}$	vector of input values
R_1, R	bearing radius (m)
R_2	journal radius (m)
U	linear velocity at the shaft surface (m/s)
$\underset{w}{\rightarrow}$	vector of weights
x	x-variable of cartesian coordinates
y	y-variable of cartesian coordinates
yx	misalignment angle on the x-axis (rad)
yy	misalignment angle on the y-axis (rad)
Z	dimensionless z-variable $Z = z/L$
z	z-variable of cartesian & cylindrical coordinates

Greek symbols

a	output of activation function
ε_0	relative eccentricity $\varepsilon_0 = e_0/c$ at z=0
η	lubricant viscosity (Pa s)
θ	variable of cylindrical coordinates
φ_0	attitude angle (rad)